Consistency of absorbed dose to water measurements using 21 ion-chamber models following the AAPM TG51 and TG21 calibration protocols

Ramesh C. Tailor, William F. Hanson, Nathan Wells, and Geoffrey S. Ibbott
MD Anderson Cancer Center, University of Texas, Houston, Texas 77030

(Received 2 November 2004; revised 4 April 2006; accepted for publication 4 April 2006; published 25 May 2006)

In 1999, the AAPM introduced a reference dosimetry protocol, known as TG51, based on an absorbed dose standard. This replaced the previous protocol, known as TG21, which was based on an air kerma standard. A significant body of literature has emerged discussing the improved accuracy and robustness of the absorbed dose standard, and quantifying the changes in baseline dosimetry with the introduction of the absorbed dose protocol. A significant component playing a role in the overall accuracy of beam output determination is the variability due to the use of different dosimeters. This issue, not adequately addressed in the past, is the focus of the present study. This work provides a comparison of absorbed dose determinations using 21 different makes and models of ion chambers for low- and high-energy photon and electron beams. The study included 13 models of cylindrical ion chambers and eight models of plane-parallel chambers. A high degree of precision ($<0.25\%$) resulted from measurements with all chambers in a single setting, a sufficient number of repeat readings, and the use of high quality ion chambers as external monitors. Cylindrical chambers in photon beams show an improvement in chamber-to-chamber consistency with TG51. For electron dosimetry with plane-parallel chambers, the parameters N_{gas} and the product $N_{D,w}\cdot k_{\text{ecal}}$ were each determined in two ways, based on (i) an ADCL calibration, and (ii) a cross comparison with an ADCL-calibrated cylindrical chamber in a high-energy electron beam. Plane-parallel chamber results, therefore, are presented for both methods of chamber calibration. Our electron results with technique (i) show that plane-parallel chambers, as a group, overestimate the beam output relative to cylindrical chambers by 1%–2% with either protocol. Technique (ii), by definition, normalizes the plane-parallel results to the cylindrical results. In all cases, the maximum spread in output from the various cylindrical chambers is $<2\%$ implying a standard deviation of less than 0.5%. For plane-parallel chambers, the maximum spread is somewhat larger, up to 3%. A few chambers have been identified as outliers. © *2006 American Association of Physicists in Medicine*. [DOI: 10.1118/1.2199598]

Key words: TG21, TG51, ion chambers, plane-parallel chambers, cylindrical ion chambers

I. INTRODUCTION

The calibration protocol [TG51 (Ref. 1)], currently recommended by the AAPM, was presented in 1999. Currently the Radiological Physics Center (RPC) remotely monitors beam outputs and electron depth doses of nearly 1400 institutions participating in NCI-conducted clinical trials. Based on the RPC's mailed TLD records, as of January 2006, 78% of these institutions have switched from the previously recommended TG21 (Ref. 2) protocol to the current TG51 protocol. Various objectives of the new protocol, improving accuracy and simplifying implementation, etc., have been addressed in the literature. What has remained obscure is the variation in output arising from the use of different makes and models of ion chambers (see, for example, Seuntjens *et al.*[3]). The object of this work is to address this issue.

High precision (standard deviation of 0.25%) relative output calibration results using both protocols are presented for a wide range of ion chamber models: 13 cylindrical (cyl) and eight plane parallel (PP). The study includes both photon and electron beams at representative low (6 MV, 6 MeV) as well as high (18 MV, 16 MeV) energies.

The ADCLs provide chamber calibrations at ^{60}Co in terms of N_K (N_X) for TG21 and $N_{D,w}$ for TG51. In 1994, the AAPM task group report, TG39 (Ref. 4) recommended a cross-comparison technique in a high energy electron beam for plane-parallel ionization chambers, which had already been suggested in TG21. This technique is strongly recommended in TG51. Cross-calibration provides chamber calibration in an electron beam in terms of the quantity N_{gas} for TG21 and the product $N_{D,w}\cdot k_{\text{ecal}}$ for TG51. PP results are presented here using both the ^{60}Co calibration and the cross calibration in an electron beam.

Several interesting and important conclusions emerge from this study. Agreement among cylindrical chambers with TG51 is better than the agreement with TG21 for photons. With TG51, there is very good agreement at 6 MV and somewhat less good agreement at 18 MV. For photons with TG21 and for electrons with both protocols, agreement

among the various cylindrical chambers is not as good. The results for PP chambers are somewhat more complicated because of the two chamber-calibration techniques. The cross-calibration technique matches output for electrons determined by the PP chambers to that determined by the specific cylindrical chamber used for the cross calibration at 16 MeV. Our results will show how well the agreement holds as the electron beam energy changes. There is a systematic discrepancy between the PP and cylindrical chamber results for both electrons and photons (TG21 only) when the ADCL ^{60}Co calibration technique is used. For photons with TG21, the discrepancy is even larger using the cross-calibration technique.

II. MATERIALS AND METHODS

To evaluate the differences in beam-output measurements with different ion chambers, the output was measured in several photon and electron beams under carefully controlled conditions. All measurements were converted to dose using the current TG51 protocol and the earlier TG21 protocol. Twenty-one different makes and models of ionization chambers were used in these measurements. Both cylindrical (13) and plane-parallel (8) chambers were used. The intent was to measure beam output with all of the currently popular chambers, and a number of recently designed chambers. The chambers are listed in Table I. The table also lists the characteristics of the chambers.

All chambers were calibrated at the MD Anderson Cancer Center ADCL during the period over which these measurements were made. Both the exposure calibration coefficient (N_X) for TG21 and the dose to water calibration coefficient ($N_{D,w}$) for TG51, were assigned by the ADCL. PP chambers were calibrated using the techniques currently in use at the MDACC ADCL. For N_X the chambers were calibrated in air with no additional scatter other than adequate buildup, with the point of measurement defined to be the center of the air cavity. For $N_{D,w}$, PP chambers were calibrated in a liquid water phantom with the effective point of measurement defined to be the distal surface of the front window. The PP chambers were also calibrated by cross comparison, with an ADCL-calibrated NEL Model 2571 Farmer chamber in the 16 MeV electron beam in water during the actual data taking. Throughout this presentation we call this the "calib in e^- beam" technique.

Accumulated charge was measured with as many as 5 electrometers, which were simultaneously controlled and read by custom software (see "Acknowledgment" section). All electrometers were calibrated by the MDACC ADCL. Data were continuously displayed graphically in real time on a computer screen. These data were continuously observed and data capture continued until all chambers stabilized (typically 0.02% at 1 σ). The electrometers used included multiple Keithley model-617s and a Keithley model-602, interfaced to a Fluke digital voltmeter. The electrometers were automatically zeroed, the beginning reading recorded, the accelerator run for 50 mu (in most cases), and the final accumulated charge recorded. A single Varian Clinac 2100CD (Varian Associates, Palo Alto, CA) at M.D. Anderson Cancer Center (MDACC) was employed for all measurements. Both low and high energy photon (6 and 18 MV) and electron (6 and 16 MeV) beams were measured with a nominal dose rate of 400 mu/min. Table II lists the important characteristics of the four therapy beams.

At least one, and usually two, external ion chamber monitors, located off-axis, were used to normalize the data. For photons, the monitors were located at 20 cm depth while for electrons the monitors were located at 1.4 cm depth, near maximum ionization for both 6 and 16 MeV beams. For measurements of P_{ion} and P_{pol}, the monitor chamber was located at the same depth as the test chamber(s). The use of external monitor chambers reduced uncertainty due to machine fluctuations by a factor of 5 to 10, depending on the beam.

All dose measurements were made in a 30 cm $\times$ 30 cm $\times$ 30 cm water phantom using a horizontal beam, at 100 cm SSD. For convenience, P_{ion} and P_{pol} were measured in a PMMA (Lucite, acrylic) phantom. The assumption is that P_{ion} and P_{pol} are independent of phantom material when the field size, dose rate, and geometry are maintained. A field size of 15 cm $\times$ 15 cm provided sufficient margins for the monitors for all beams.

For additional redundancy, the first chamber (an NEL-2571 or Exradin A-12), measured at the start of a session, was remeasured at the end of the session. The reproducibility between the start and the end measurements of each lengthy session was typically 0.1% and occasionally reached up to 0.2%.

Through the use of a pin-hole light source and scribe marks on the phantom, a precision micrometer drive and precision pointers, the depth determination from chamber to chamber was reproducible to $\approxeq$ 0.2 mm. For photons, TG51 measurements were made at 10.0 cm depth, and TG21 measurements were made at 5.0 and 7.0 cm depths for the 6 and 18 MV beams, respectively. For electrons, we chose to measure ionization at d_{ref} because that is the depth required by TG51. Although TG21 recommends measurement at $d_{\max}$, it provides data to calculate dose at any depth. For both photons and electrons, the depth dose values required for transferring the dose to $d_{\max}$, were measured and calculated following the strict guidelines of the two protocols. This required the use of protocol-dependent stopping power ratios for electrons and different displacement corrections (shift) for both modalities. Measurements of P_{ion} and P_{pol} were made at 8 cm depth for photons and at d_{ref} for electrons. Depth dose, and beam-quality specifiers [$\text{TMR}_{20/10}$, $\%\text{dd}(10)_x$, and I_{50}] were measured one time on each beam using a Farmer chamber for photons and a plane-parallel chamber for electrons.

Wherever there are chamber-specific data in TG51 and TG21 protocols, those data were used in this presentation. For those chambers for which data are not provided in the protocols, we have used the recommended procedures in the protocols for obtaining data for unlisted chambers. In some

TABLE I. Chamber identification and specifications. The table also includes ADCL calibration coefficients, N_{gas}/N_X, and k_{ecal} for each chamber.

	Ion chamber					Collector			Wall/Front window					
Chamber ID	Make	Model	Volume [cc]	^{60}Co Build-up cap	ID [mm]	Mat [mm]	Dia [mm]	L[a]/Gap [mm]	Material	[mm]	N_{gas}/N_X [cGy/R]	k_{ecal}	$N_{D,w}$ [10^7 Gy/C]	N_X [10^9 R/C]
	Cylindrical													
1	NEL	2571	0.60	3.87 mm Delrin	6.3	Alum	1.0	22.5	Gr	0.360	0.854	0.903	4.53	4.69
2	PTW	23333	0.60	4.60 mm PMMA	6.1	Alum	1.0	21.9	PMMA/Gr	0.335/0.089	0.849	0.897	5.31	5.51
3	PTW	30001	0.60	4.60 mm PMMA	6.1	Alum	1.1	23.0	PMMA/Gr	0.335/0.090	0.849	0.897	5.28	5.49
4	PTW	30013	0.60	4.55 mm PMMA	6.1	Alum	1.1	23.0	PMMA/Gr	0.335/0.090	0.849	0.897	5.35	5.54
5	PTW	30004	0.60	4.60 mm PMMA	6.1	Alum	1.0	23.0	Gr	0.425	0.854	0.905	5.05	5.24
6	PTW: CNMC version	30004.2	0.20	4.60 mm PMMA	6.1	Alum	1.0	8.0	Gr	0.425	0.851	0.905	18.76	19.45
7	PTW	233641	0.30	3.00 mm PMMA	5.5	Alum	1.5	16.3	PMMA/Gr	0.750	0.850	0.898	9.75	10.06
8	Capintec	PR-06C	0.65	5.16 mm Polyst	6.4	C552[c]	1.6	23.0	C552[c]	0.280	0.851	0.900	4.73	4.90
9	Capintec	PR-06G	0.65	5.16 mm Polyst	6.4	C552[c]	1.6	23.0	C552[c]	0.280	0.851	0.900	5.02	5.22
10	Exr/Std.Im	A-12	0.65	2.80 mm C552[c]	6.1	C552[c]	1.0	24.1	C552[c]	0.500	0.866	0.906	5.03	5.19
11	Scanditronix/WellHofer	IC-70	0.65	3.90 mm Delrin	6.2	Alum	1.0	23.1	Gr	0.400	0.854	0.903	4.81	4.97
12	Scanditronix/WellHofer	FC65-P	0.65	3.90 mm Delrin	6.2	Alum	1.0	23.1	Delrin	0.400	0.850	0.899	4.87	5.03
13	Scanditronix/WellHofer	FC23-C	0.23	3.90 mm Delrin	6.2	C552[c]	1.0	8.8	C552[c]	0.400	0.856	0.903	14.48	14.96
	Plane-parallel													
14	PTW Markus	23343[b]	0.06	3.2 mm PMMA	5.3	PMMA	5.3	2.0	Polyeth/Gr	0.03	0.859	0.905	54.7	55.1
15	PTW Adv-Markus	34045[b]	0.02	3.2 mm PMMA	5.0	PMMA	5	1.0	Polyeth/Gr	0.03	0.856	0.896	140.6	141.2
16	PTW Roos	34001	0.35	3.2 mm PMMA	15.6	PMMA	15	2.0	PMMA/Gr	1.00	0.855	0.901	8.30	8.37
17	Exr/Std.Im	P-11	0.62	4.0 mm Polyst	20.0	Polyst-eq	20	2.0	Polyst-eq/Gr	1.00	0.848	0.888	5.88	5.86
18	Exr/Std.Im	A-10[b]	0.05	2.81 mm C552[c]	5.4	C552[c]	5.4	2.0	Kapton/Gr	0.03	0.870	0.939	60.6	62.4
19	Scanditronix/Wellhofer	NACP-02	0.16	2.31 mm Graph	10.0	Rexolite	10	2.0	Mylar/Gr	0.1/0.5	0.845	0.885	17.34	17.23
20	Scanditronix/Wellhofer	PPC-40	0.40	3.2 mm PMMA	16.0	PMMA	16	2.0	PMMA/Gr	1.00	0.855	0.901	9.20	9.24
21	Scanditronix/Wellhofer	PPC-05	0.05	2.04 mm C552[c]	9.9	C552[c]	9.9	0.6	C552[c]	1.00	0.873	0.896	58.6	59.4

[a]Active volume's length (L) for cylindrical chambers, and plate separation (Gap) for parallel-plate chambers.
[b]PMMA caps (water protective): 0.85, 0.87, and 1.00 mm thick for chambers Nos. 14, 15, and 18, respectively.
[c]Air-equivalent conducting plastic.

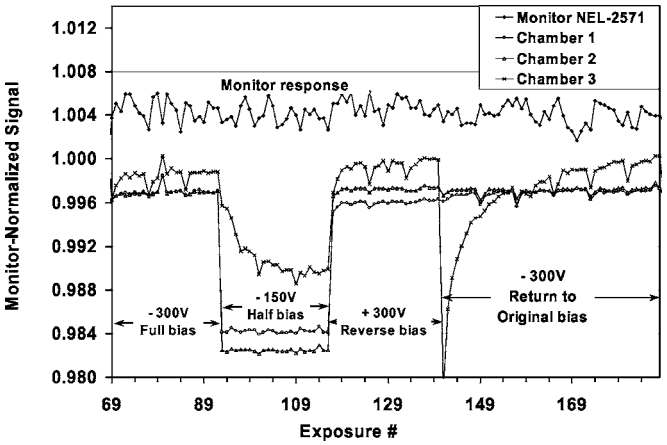

FIG. 1. Sample data-capture. Data for the determination of P_{ion} and P_{pol} in a 16 MeV electron beam for three models of Farmer-type chambers. The upper curve shows the accumulated charge of the monitor chamber. The other plots are the accumulated charge of each sample chamber normalized to the monitor chamber. The indicated biases are the polarizing voltages on the thimble. The bias is cycled through full voltage, half voltage, reverse voltage, returning to the original full voltage. Each exposure represents 50 mu. Note: In order to display all data simultaneously during data acquisition; an arbitrary normalization was additionally applied.

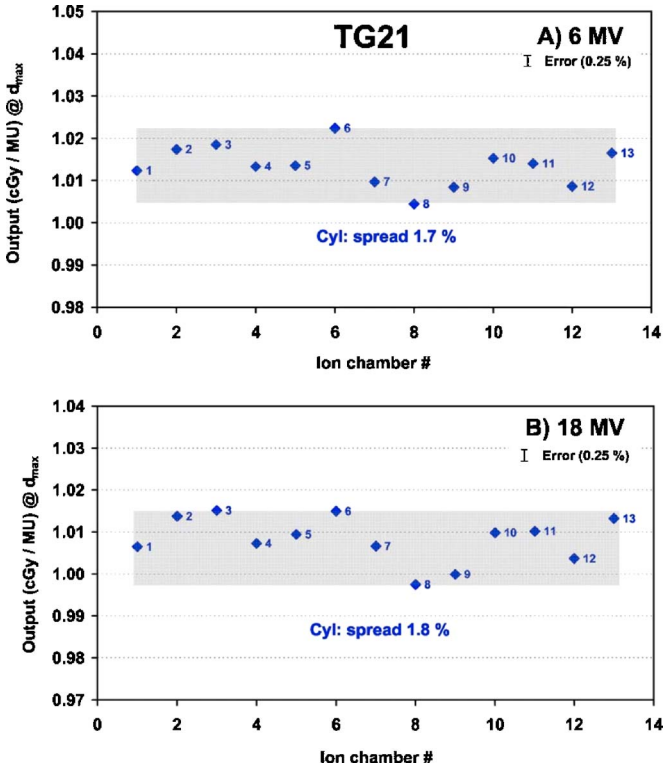

FIG. 2. Cylindrical-chamber results of TG21 output for 6 MV (A) and 18 MV (B) photon beams. The values are the measured output normalized to the monitor chamber(s). The shaded area represents the maximum-to-minimum distribution among the chambers.

cases where data for unlisted chambers were presented elsewhere, we have used those data. The sources of the data are provided in the section on "Assumptions."

The emphasis of this study is to compare various chambers in the same beam using a single protocol rather than to determine the protocol ratio (TG51/TG21).[5] Therefore a measurement session consisted of a single beam and a single protocol irradiating all chambers. When viewing the figures and tables, the reader should focus on the relative output values from chamber to chamber, rather than on the absolute values of the output. Our external monitoring system enabled us to tie (normalize) all data to the dose rate determined by chamber No. 1 (NEL 2571) on the first day of measurements, using TG51. This did not necessarily measure 1.000 cGy/mu on any beam.

The astute reader may wish to determine the TG51/TG21 ratio from our data. We do not recommend this, but refer the reader to our previous theoretical publication.[5] If you wish to do this, you must be careful to consider at least the following issues. To compare doses at d_{max}, depth dose comes into play; which may be different for the two protocols for both modalities due to differences in stopping powers and the shift to the effective point of measurement. Differences in beam qualities would also affect the TG51/TG21 ratio between our data and other authors. Some chambers in this paper use updated values of N_{gas}/N_X and k_{ecal} (chambers Nos. 16, 19, and 20). Last, NIST has changed the air kerma standard in 2003 (all of our chambers were calibrated with the pre-2003 air kerma standard). Even though these issues do not change the chamber-to-chamber variations within a given protocol, as a redundant check of our data we verified that, considering these issues, we reproduced our previously published TG51/TG21 (Ref. 5) values.

III. ASSUMPTIONS

A basic assumption of this study is that chambers of the same make and model would reproduce our results within

TABLE II. Beam characteristics: Beam-energy specifier, measurement depth, and fractional depth-dose data for the four photon and electron beams used.

Beam	$TMR_{20/10}$ or I_{50}/R_P	$\%dd(10)_X$ or R_{50}	Measurement depth[a] (cm) TG21	Measurement depth[a] (cm) TG51	fdd[b] TG21	fdd[b] TG51
Photons (6 MV)	0.674	66.3%	5	10	0.868	0.663
Photons (18 MV)	0.785	81.4%	7	10	0.920	0.806
Electrons (6 MV)	2.6/3.4 cm	2.6 cm	1.4_5	$d_{ref}=1.4_5$	0.999	1.000
Electrons (16 MV)	6.4/8.0 cm	6.5 cm	3.8_0	$d_{ref}=3.8_0$	0.994	0.992

[a]Depth of cylindrical chamber's axis, or inner surface of entrance window of parallel-plate chamber.
[b]The symbol "fdd" stands for fractional depth dose.

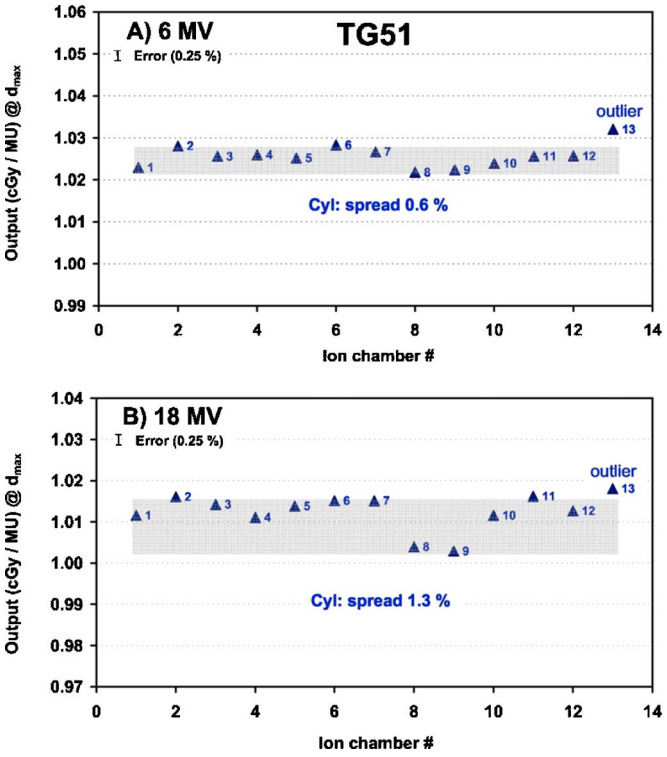

FIG. 3. Cylindrical-chamber results of TG51 output for 6 MV (A) and 18 MV (B) photon beams. The outlier, as indicated is defined in the text.

our measurement uncertainty. We did not address this issue directly. However, for various reasons we were forced to use two different chambers for each of three models during the course of our work. These limited data showed 0.3% maximum variation between two chambers of the same model. These results are similar to the variability reported by Seuntjens *et al.*[3] who measured k_Q values using as many as five chambers of the same model.

A number of chambers in this study were not in production when TG21, TG39, and TG51 were written, so pertinent data for some chambers were not included in the protocols. These pertinent data include N_{gas}/N_X for TG21, and k_{ecal} for TG51. It was necessary for us to make the assumptions listed below about the specified chambers. These assumptions introduce additional uncertainties. For chambers that were not specially addressed in the protocols, we followed the recommendations made by both protocols to identify an equivalent chamber for protocol parameters. We have not quantified the additional uncertainty; however, it is reflected as variability in the results, and is representative of community practice.

Chamber Nos. 2–4 (PTW cylindrical): TG51 provides data for chamber No. 3 (PTW N30001) but not for chamber No. 2 (PTW N23333). The two chambers are identified to be identical by the manufacturer. In addition, chamber No. 4 (PTW N30013) is identified by the manufacturer to be the waterproof version of N30001. We have assumed that these chambers are in fact equivalent.

Chamber Nos. 5 and 6 (PTW cylindrical): TG51 provides data for chamber No. 5 (PTW N30004). The manufacturer of chamber No. 6 (N30004-2) claims it to be identical to chamber No. 5 except for the thimble length. We have assumed them to be equivalent.

Chamber No. 11 (cylindrical IC-70): The chamber has dimensions and materials very similar to the NEL model 2571. We have used values for the model 2571.

Chamber No. 12 (cylindrical FC 65-P): Both thimble and build-up cap are constructed of Delrin, but neither protocol has adequate data to calculate N_{gas}/N_X, P_{wall}, k_Q or k_{ecal}. Values of $\bar{L}/\rho|^{delrin}_{air}$, $\bar{\mu}_{en}/\rho|^{water}_{delrin}$, and P_{cel} are required. These data were obtained from the IAEA technical report series 277 (TRS-277) (Ref. 6) and Rogers.[7] Values of k_{ecal} and k_Q were calculated using equations provided by Rogers.[7,8]

Chamber No. 13 (cylindrical FC23-C): This chamber has a C552 wall thickness between that of chambers Nos. 9 and 10 (PR-06G and A-12). Therefore, k_{ecal} was set equal to the average for chamber Nos. 9 and 10.

Chamber No. 15 (PP N34045 "adv markus"): The k_{ecal} value was taken from Mainegra-Hing *et al.*[9]

Chamber No. 18 (PP A-10): The k_{ecal} value was taken from Mainegra-Hing *et al.*[9] For this presentation, the chamber was calibrated with a C552 buildup plate, and N_{gas}/N_X calculated following Nath and Schulz[10] for the C552 wall.

Chamber No. 19 (PP NACP-02): The k_{ecal} value was taken from Mainegra-Hing *et al.*[9] The body of this chamber is Rexolite (polystyrene like material) while the front window is thin mylar with 0.5 mm graphite. We calibrated the chamber with both graphite and polystyrene buildup slabs and calculated N_{gas}/N_X for both conditions following Nath and Schulz.[10] The measured N_X values were the same (within 0.1%) for both slabs while our calculated N_{gas}/N_X values for the two slabs differed by 0.7%. However our calculated N_{gas}/N_X value with the graphite buildup slab is 2.1% larger than the TG39 value (graphite buildup). In this presentation we used the N_X value for the graphite slab and the N_{gas}/N_X value from TG39.

Chamber Nos. 20 and 21 (Scanditronix-Wellhofer PPC-40 and PPC-05): On advice from the manufacturer, we assumed these chambers to be equivalent to PTW Roos, Model 34001 (chamber No. 16) and PTW Advanced Marcus, Model 34045 (chamber No. 15), respectively.

IV. SOURCE FOR N_{gas}/N_X AND P_{wall} VALUES

Values of N_{gas}/N_X were taken from Gastorf *et al.*[11] for cylindrical chambers and from TG39 (Ref. 4 for PP chambers, if possible. The remainder were calculated using Nath and Schulz.[10] Values of P_{wall} for PP chambers were calculated based on the materials and thickness of the front wall, the general practice for TG21.

V. RESULTS AND DISCUSSION

Figure 1 illustrates the data capture method. Shown are data to determine P_{ion} and P_{pol} simultaneously for three different makes and models of Farmer type ion chambers. Each data point is the accumulated charge for a 50 mu exposure, normalized to the external monitor. In the subsequent text, this will be referred to as "normalized signal." The monitor

signal is the upper curve. The readings were repeated until the normalized signal stabilized for all chambers in the setup. Our aim for stability was nontrending data with a spread (max/min) of <0.02%. For most chambers we were able to attain this level of stability. However, occasionally, chambers did not reach this level (e.g., chamber No. 3 in Fig. 1). Typically the average of the last five readings in the stabilized region was used in the calculations. A few comments with regard to Fig. 1 are worth mentioning:

(i) We determined the small spikes to be an anomaly in our measurement technique and ignored them.
(ii) One chamber shows P_{ion} substantially nearer unity than the other two. This is expected since this chamber has a substantially larger diameter central electrode.
(iii) For P_{ion} and P_{pol} measurements, the chambers were finally returned to the original bias (−300 V on the thimble) to assure that they reproduced their original signal.
(iv) Two of these chambers stabilized very quickly and returned to the original signal, while one chamber took unusually long (~30 repeats of 50 mu) to stabilize, and exhibited nearly 0.2% drift with respect to the original signal at −300 V. This figure shows the behavior typical of the best and the worst behaving chambers.

Figures 2–9 show beam output determined for a variety of chambers. In the figures the shaded area is the range from maximum to minimum output for the cluster of data. Usually this area is less than ±2 standard deviations of the data in the cluster. There are three chambers that obviously behave differently from others in at least one data set. We identified them as outliers based on the following criterion. A chamber was identified as an outlier if the measured output fell outside two standard deviations from the mean in one of the data sets. The same chamber, in other data sets, continued to be treated as an outlier if it fell outside the shaded area. Chamber No. 13 met the outlier criterion in Figs. 3(A), 6(A), 7(A), 8(A), and 9(A), and was treated as an outlier in Figs. 3(B), 6(B), 7(B), 8(B), and 9(B) also. Chamber No. 18 met the outlier criterion in Figs. 6(A) and 7(A). Chamber No. 21 met the outlier criterion in Figs. 5(A), 5(B), 6(A), 7(A), 8(A), and 8(B), and was treated as an outlier in Fig, 9(A) also.

A. Photons

Figures 2(A) and 2(B) show TG21 output for 6 and 18 MV photons, respectively, determined with cylindrical chambers, the most common chambers used for photon beam calibration. The corresponding TG51 results are presented in Figs. 3(A) and 3(B). With 6 MV x rays, the agreement for TG51 output among the 13 cylindrical chambers was strikingly tight (0.6% spread) with one outlier (−0.6% away from the mean). At 18 MV for TG51, the spread was almost doubled (1.3%). However, the two chambers at the lower end of the distribution are Capintec PRO6C and PRO6G chambers (No. 8 and No. 9). At this energy, Seuntjens *et al.*[3] measured k_Q for the Capintec chamber to be 0.7% higher than the value reported in TG51. That would make the 18 MV distribution as tight as that at 6 MV. TG21 spreads for photon beams were larger than those for TG51 (1.7%–1.8%) at both energies. Chamber No. 13 was identified as an outlier based primarily on electron results.

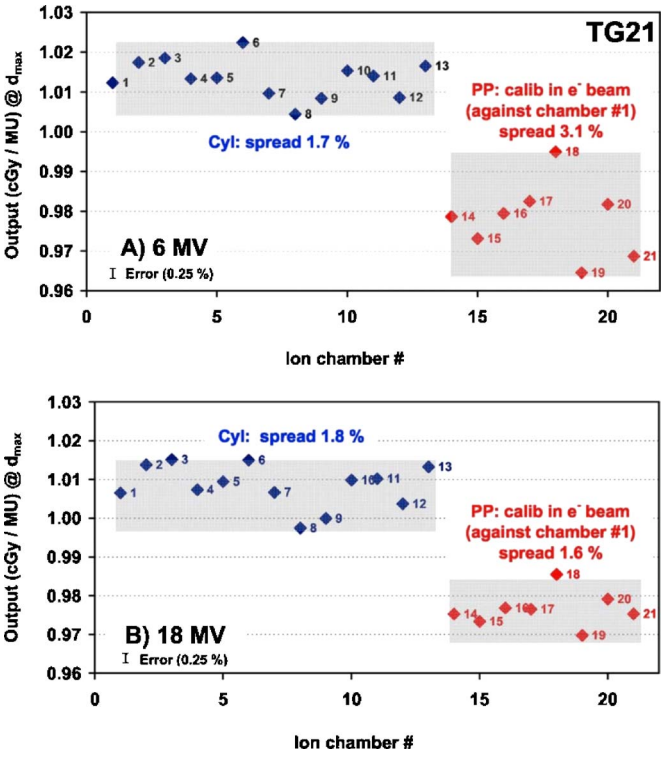

FIG. 4. Plane-parallel chamber results of TG21 output for 6 MV (A) and 18 MV (B) photon beams, using "calib in e⁻ beam" for PP chambers. All eight plane-parallel chambers were calibrated against chamber No. 1 in the 16 MeV electron beam. The cylindrical results are repeated here to emphasize the systematic difference in output obtained with the two chamber types.

The differences in the spread may be explained by the following argument. For TG51, the uncertainties in chamber construction-dependent corrections at ^{60}Co are absorbed in $N_{D,w}$. The energy dependent component of these uncertainties is contained in k_Q; so at beam energies near ^{60}Co (6 MV) we expect tight agreement. The energy dependent uncertainties express themselves more at the higher energy (spread increases from 0.6% to 1.3%), as shown by measurements.[3] In TG21, the chamber-construction dependent parameters, at ^{60}Co, are explicitly contained in N_{gas}/N_X. The lack of understanding of these parameters contributes to a significant uncertainty in N_{gas}/N_X. This is reflected as the difference between our TG51 and TG21 results.

TG21 allows calibration of photon beams with PP chambers, while TG51 does not. For the use of PP chambers with TG21, the Task Group 39 report[4] describes two calibration methods, "^{60}Co calib" and "calib in e⁻ beam." TG21 photon results with PP chambers are presented in Figs. 4 and 5. The PP chambers employing the user's calibration "calib in e⁻ beam" are presented in Figs. 4(A) and 4(B). The correspond-

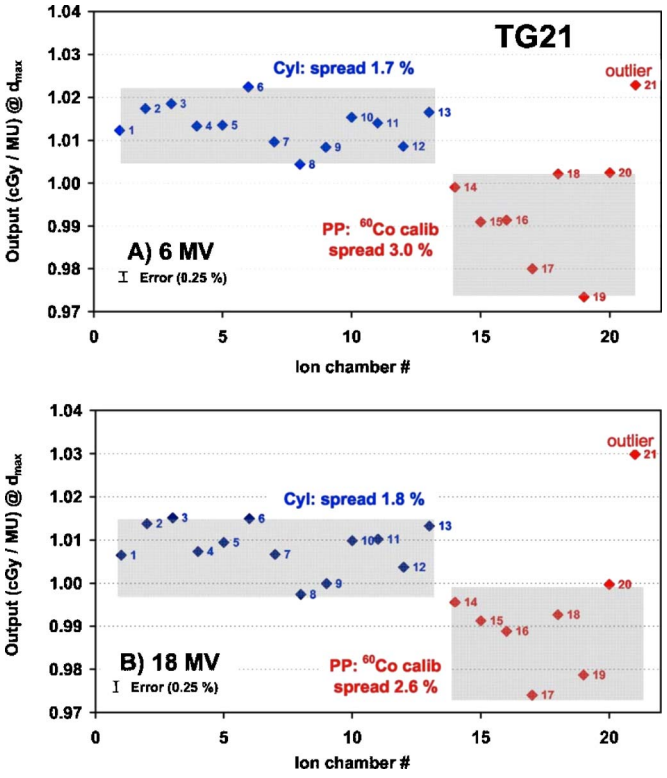

FIG. 5. Plane-parallel chamber results of TG21 output for 6 MV (A) and 18 MV (B) photon beams. The plane-parallel chambers were calibrated by the ADCL in a ^{60}Co beam. Again, the cylindrical results emphasize the systematic difference in output obtained with the two chambers types.

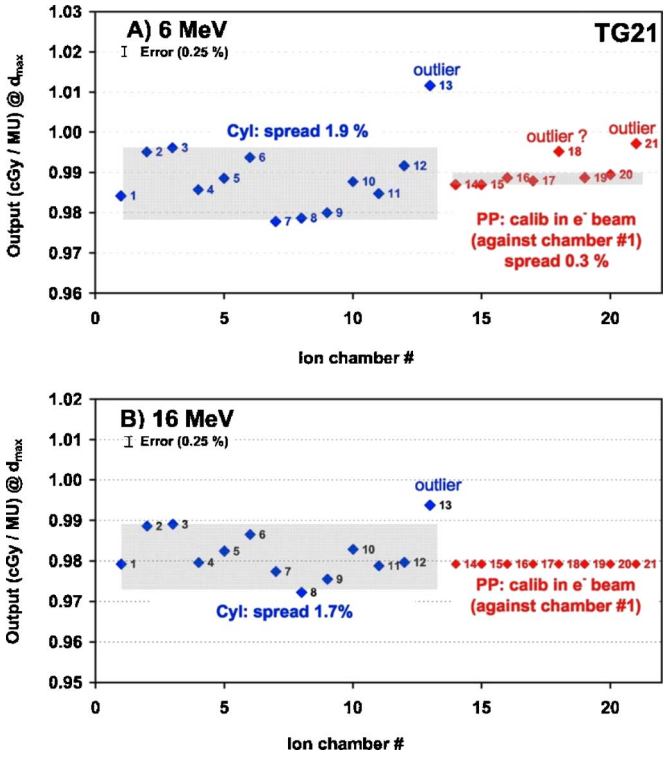

FIG. 6. Electron output using TG21 for both plane-parallel and cylindrical chambers at 6 MeV (A) and 16 MeV (B). The calibration of the plane-parallel chambers is based on cross calibration with chamber No. 1 in the 16 MeV electron beam.

ing PP results employing ^{60}Co calibrations are shown in Figs. 5(A) and 5(B). The TG21 PP results for photons deserve the following comments.

With "^{60}Co calib," at both photon energies [Figs. 5(A) and 5(B)], the average output measured with PP chambers was 2%–2.5% lower than the average TG21 output determined with cylindrical chambers. With "calib in e^- beam," TG21 output measured with PP chambers was an additional 1% lower (3%–3.5%) as seen in Figs. 4(A) and 4(B). The spread among PP chamber results with "calib in e^- beam" [Figs. 4(A) and 4(B)], at 18 MV was comparable to that among cylindrical chamber results (~1.5%). However at 6 MV, the 3.1% spread for PP chambers was almost twice that for cylindrical chambers. With "^{60}Co calib" [Figs. 5(A) and 5(B)], the spread among PP chamber results was larger than that among cylindrical chamber results at both photon energies.

Chamber No. 21 was clearly an outlier from all other ^{60}Co-calibrated PP chambers [Figs. 5(A) and 5(B)]. It was also an outlier for electrons as will be seen in the following section.

B. Electrons

Figures 6(A) and 6(B) give the TG21 output results (absorbed dose at d_{max}) for 6 and 16 MeV electrons using ^{60}Co calibration for cylindrical chambers and "calib in e^- beam" for PP chambers. The corresponding TG51 results are shown in Figs. 7(A) and 7(B). Figures 8(A) and 8(B) give similar TG21 electron results, employing the ^{60}Co calibration for both PP and cylindrical chambers. Figures 9(A) and 9(B) give the corresponding TG51 results. For easier comparison, cylindrical chamber results using only "^{60}Co calib" are included in all Figs. 6–9.

The spread among the cylindrical chamber results was the same (1.7%–1.9%) for both protocols at both energies and was comparable to cylindrical chamber results in photon beams using TG21. As stated earlier in the photon discussion, the uncertainty in chamber-dependent parameters is eliminated only for TG51 at ^{60}Co energy. For electrons, these parameters reenter through k_{ecal} for TG51 and N_{gas}/N_X for TG21.

Cylindrical chamber No. 13 appears to be an outlier for both protocols and at both energies. The fact that it is constructed of air-equivalent plastic (C552) did not appear to explain the large discrepancy. None of the other chambers constructed of C552, namely chambers Nos. 8, 9, and 10, was an outlier.

For PP chambers, the calibration in an e^- beam was obtained by comparison with chamber No. 1 in our 16 MeV beam. Therefore, by definition, all PP results at 16 MeV for both protocols agreed exactly with chamber No. 1 when the "calib in e^- beam" technique was used. At 6 MeV, the spread among PP chamber results was 0.3% for both protocols, which is close to the measurement uncertainty. Chamber Nos. 18 and 21 were notable outliers for both protocols, and

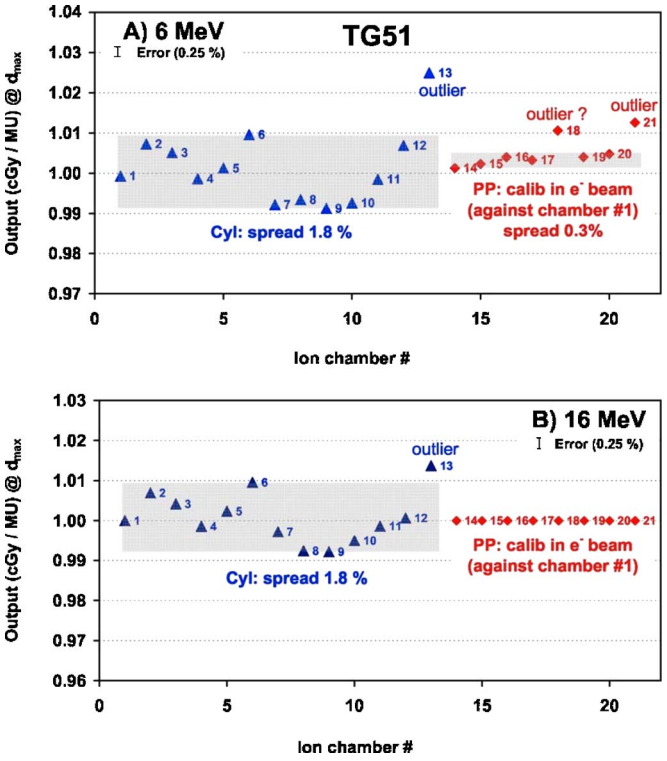

FIG. 7. Electron output using TG51 for both plane-parallel and cylidrical chambers at 6 MeV (A) and 16 MeV (B). The calibration of the plane-parallel chambers is based on cross calibration with chamber No. 1 in the 16 MeV electron beam. The narrow shaded area over the plane-parallel data is artificial because it is based on comparison with chamber No. 1 alone. The actual spread for the plane-parallel chambers is the sum of the spreads over both cylindrical and plane-parallel chambers.

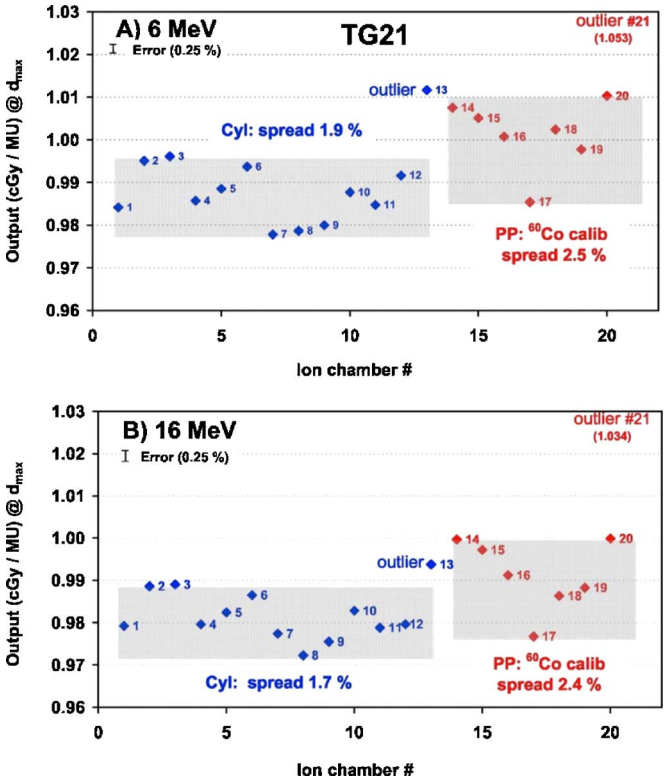

FIG. 8. Electron output using TG21 for both plane-parallel and cylindrical chambers at 6 MeV (A) and 16 MeV (B). The cylindrical chamber data are repeated from Fig. 6, to facilitate comparison with the plane-parallel results. The plane-parallel chambers are calibrated by the ADCL in a ^{60}Co beam. The outlier (chamber No. 21), is outside the bounds of the figure.

it was noted that both were constructed of air-equivalent conducting plastic (C552). To fully appreciate the total spread in the expected output with PP chambers, using the "calib in e$^-$ beam" technique, we must consider that these chambers could have been compared with any of the cylindrical chambers, and therefore the apparent spread in the PP chambers at 6 MeV must be compounded with the spread in the cylindrical-chamber data at 16 MeV.

One concern against the use of cylindrical chambers for low energy electrons is their spatial resolution in the region of the sharp peak in the depth dose curve. This would result in the underestimation of beam output by cylindrical chambers at the lower energies. For both protocols, using the "calib in e$^-$ beam" technique [Figs. 6(A) and 7(A)], the average of PP results at 6 MeV (ignoring chambers Nos. 18 and 21) was minimally higher (0.4%) than the output determined from the cylindrical chamber No. 1 (employed for the cross calibration), consistent with this concern. We should note that we expect approximately this same deviation irrespective of which cylindrical chamber is employed for "calib in e$^-$ beam." This becomes clear when we note that the relative output of all cylindrical chambers is very similar at 6 and 16 MeV with either protocols [compare Figs. 6(A) and 6(B) or 7(A) and 7(B)].

With the "^{60}Co calib" technique, PP results at both energies with either protocol showed, on average, 1%–1.5% higher output than that obtained with cylindrical chambers. In both Figs. 8 and 9, the spread in the output data was just less than 2% for cylindrical chambers while PP chambers showed an additional 0.5% spread. The PP chamber spread, however, was controlled by chamber No. 17. When chamber No. 17 was excluded from the analysis, the spread of the PP chamber data was marginally smaller than that for cylindrical chambers.

Note that the data point for chamber No. 21 is completely off the scale for TG21 using the "^{60}Co calib" technique (see Fig. 8). For chamber Nos. 17 and 21, comparison of results based on "^{60}Co calib" versus those based on "calib in e$^-$ beam" suggests significant uncertainty in the determination of N_{gas}. The process of "calib in e$^-$ beam" enables direct empirical determination of the two quantities: chamber-calibration coefficient N_{gas} for TG21, and the product $N_{D,w} \bullet k_{\text{ecal}}$ for TG51. These two quantities can also be determined for the "^{60}Co calib" technique. The quantity N_{gas} was determined from the product $N_X \bullet (N_{\text{gas}}/N_X)$, where N_X was obtained from an ADCL and N_{gas}/N_X was either calculated from an equation in TG21 (Ref. 2) or was obtained from Gastorf *et al.*[11] or from TG39.[4] The product $N_{D,w} \cdot k_{\text{ecal}}$ was calculated from $N_{D,w}$ obtained from an ADCL ^{60}Co calibration and k_{ecal} provided by the protocol. Table III lists the values of N_{gas} and $N_{D,w} \cdot k_{\text{ecal}}$ for the eight PP chambers used in the study determined both ways: from "^{60}Co calib" and from "calib in e$^-$ beam." The ratio of the two ways is also

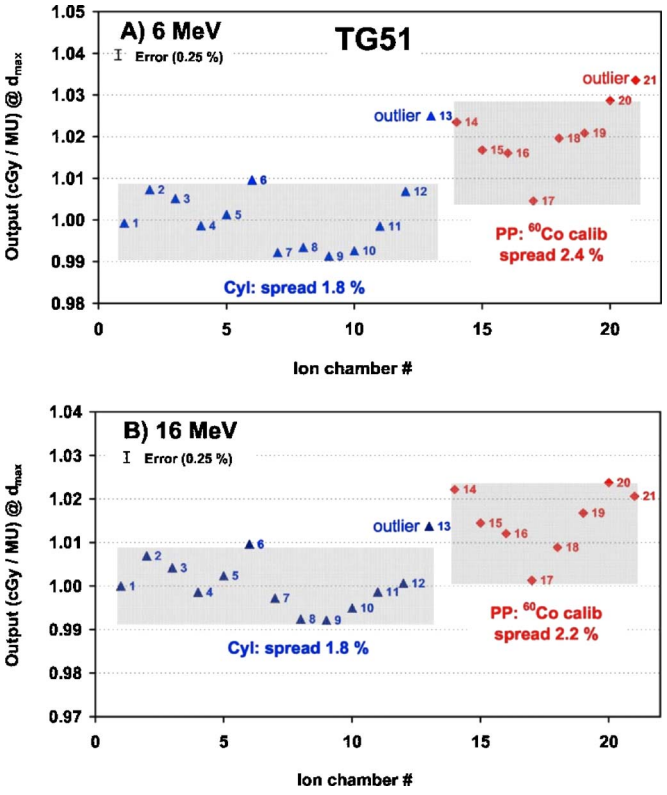

FIG. 9. Electron output using TG51 for both plane-parallel and cylidrical chambers at 6 MeV (A) and 16 MeV (B). Again, the cylindrical chamber data are repeated from Fig. 7, to facilitate comparison with the plane-parallel results. The plane-parallel chambers are calibrated by the ADCL in a ^{60}Co beam.

listed and represents the disparity between the output determined by the two methods for individual chambers. The ratios vary from 0.997–1.024 excluding the N_{gas} ratio of 1.056 for the outlier chamber No. 21.

Table IV summarizes the relative beam output results in terms of the spread among individual chambers of each class (cylindrical and PP), and the disparity in the results of the two classes of chambers. Disparity between the PP chambers and the cylindrical chambers is presented as the ratio of the median output determined by the two classes of chambers. The spread is presented for all combinations of beam energy, modality, chamber class, calibration technique (^{60}Co or e$^-$ beam), and calibration protocol (TG21 or TG51).

VI. UNUSUAL FINDINGS

(i) For one PP chamber (No. 18), P_{pol} was unusually high for electrons (2.3% for 6 MeV and 1.6% for 16 MeV). Other PP chambers showed a polarity correction of no more than 0.9%.

(ii) Several chambers took an unusually long time to stabilize, particularly during measurements of P_{ion} and P_{pol}. The worst chamber drifted as much as 2% until settling, after receiving 24 Gy (see Fig. 1). Although the time to stabilization changed from one measurement condition to another, the chambers always took a long time to stabilize.

VII. INFLUENCE OF THE RECENT CHANGE IN THE NIST STANDARD FOR AIR KERMA

All of the TG21 data are based on air kerma standards prior to the change in the NIST air kerma standard in 2003. The change is the same for all chambers, and therefore has no impact on the relative TG21 calibrations (chamber-to-chamber).

VIII. MEASUREMENT PRECISION

Aiming for a high degree of precision was an important consideration in this work. This was achieved by (i) having the MDACC ADCL perform calibrations of all the chambers in a short time span, (ii) employing monitor normalization, (iii) acquiring a large number of successive repeat measurements to ensure stabilization, (iv) using special gadgets to ensure set-up precision, (v) completing TG51 or TG21 calibration measurements of the entire set of chambers in a single session, and (vi) confirming session stability by repeating the first chamber measurement at the end of each session.

The overall uncertainty in the presented results was 0.25% at one standard deviation (1σ), as confirmed by repeat measurements with two chambers in several sessions over different days. This was consistent with an estimate obtained

TABLE III. The values of N_{gas} and the product $N_{D,w}\cdot k_{ecal}$ for the eight plane-parallel chambers using the two calibration techniques (ADCL calibration at ^{60}Co and cross comparison with a cylindrical chamber in a high-energy electron beam). The ratios "ADCL/e$^-$ beam" emphasize discrepancies between the two techniques.

	Parallel-plate ion chambers		$N_{D,w}\cdot k_{ecal}$ [10^7 Gy/C]			N_{gas} [10^9 R/C]		
Chamber ID	Make	Model	ADCL	Calib in e$^-$ beam	ADCL/e$^-$ beam	ADCL	Calib in e$^-$ beam	ADCL/e$^-$ beam
14	PTW	23343 Markus	49.5	48.4	1.022	47.3	46.3	1.021
15	PTW	34045 Adv Markus	126.0	124.2	1.014	120.9	118.7	1.018
16	PTW	34001 Roos	7.48	7.39	1.012	7.15	7.06	1.012
17	Exr/Std.Im	P-11	5.22	5.21	1.001	4.97	4.98	0.997
18	Exr/Std.Im	A-10	56.9	56.4	1.009	54.3	53.9	1.007
19	Scanditronix/Wellhofer	NACP-02	15.35	15.1	1.017	14.56	14.4	1.009
20	Scanditronix/Wellhofer	PPC-40	8.28	8.09	1.024	7.90	7.74	1.021
21	Scanditronix/Wellhofer	PPC-05	52.5	51.4	1.021	51.9	49.1	1.056

TABLE IV. Summary of results: The results in all of the figures are summarized. The spread represents maximum to minimum dispersion high-lighted by the shaded regions in the figures. The ratio, ⟨PP⟩/⟨Cyl⟩, represents the disagreement between the average plane-parallel and average cylindrical chamber results.[d]

					Low energy beam		High energy beam	
Figure	Modality	Chamber class	Calibration technique	Protocol	Spread[a] (%)	⟨PP⟩/⟨cyl⟩	Spread[a] (%)	⟨PP⟩/⟨cyl⟩
2-(A),(B)	Photons	Cyl	^{60}Co calib	TG21	1.7		1.8	
3-(A),(B)				TG51	0.6		1.3	
4-(A),(B)		PP	ln e$^-$ beam	TG21	3.1	0.966[b]	1.6	0.970[b]
5-(A),(B)			^{60}Co calib	TG21	3.0	0.979	2.6	0.982
6-(A),(B)	Electrons	Cyl	^{60}Co calib	TG21	1.9		1.7	
7-(A),(B)				TG51	1.8		1.8	
6-(A),(B)		PP	ln e$^-$ beam	TG21	0.3[c]	1.004[b]		
7-(A),(B)				TG51	0.3[c]	1.004[b]		
8-(A),(B)			^{60}Co calib	TG21	2.5	1.015	2.4	1.010
9-(A),(B)				TG51	2.4	1.019	2.2	1.014

[a]Spread implies max-to-min difference in percent.
[b]These ratios are relative to chamber No. 1 rather than to the mean value of all cylindrical chambers.
[c]This spread is deceptively low; see the section "Results of Discussion."
[d]Note: The analysis presented in this table excludes a few outlier chambers, as indicated in the figures.

by compounding the uncertainties in individual factors such as geometric setup, P_{ion}, P_{pol}, depth-dose, raw reading for calibration, etc. Monitor normalization helped to eliminate uncertainty due to changes in temperature, pressure, and beam output. The values for protocol factors and N_{gas}/N_X were assumed not to contribute to the uncertainty in the results presented here, as these uncertainties would be reflected in the spread in our results.

Since relative values (not absolute) of calibration factors (N_X,$N_{D,w}$) were important in this project, the short term precision of the ADCL was a critical parameter. This precision (1σ) was estimated to be 0.2% (all chambers were calibrated over a 2 month period). Successive repeats of ionization readings stabilized generally to 0.02% (1σ). We estimated P_{ion} and P_{pol} data to an accuracy of 0.05% (1σ), which was confirmed by repeat measurements for selected chambers over a period of 2 years. Thus the dominant factor was the reproducibility of the ADCL-assigned calibration coefficients.

IX. CONCLUSIONS

One of the issues addressed during the development of the TG51 calibration protocol was whether to continue chamber calibration at ^{60}Co or to calibrate at the beam energy and modality of practical use. Calibrating at ^{60}Co relies on our knowledge of the behavior of chambers at other megavoltage energies and modalities to assure clinically reliable beam calibrations. The variability in the beam calibration shown in this presentation is a good indicator of the limitations to our knowledge of the physics of ion chambers and ultimate limitation on accuracy of reference dosimetry. In addition, there were three chambers whose results were significantly out of line with respect to the other chambers, suggesting an additional area where we lack proper understanding of the physics of chambers or have inaccurate or incomplete information about the chamber construction. These were identified as outliers, as defined in the section "Results and Discussion," and were not included in our analyses for average and spread.

We identified three ways in which TG51 appears to improve dosimetry. (1) TG51 relies on ion chamber calibration at depth in water at ^{60}Co energy; as a result, photon beam calibrations with different chambers were mutually in better agreement using TG51 than using TG21. (2) TG51 disallows the use of plane-parallel chambers for photon calibrations. (3) TG51 makes a stronger recommendation to use "calib in e- beam" for plane-parallel chambers. These claims will be supported by some of the following conclusions.

This paragraph discusses results solely for cylindrical chambers. With TG51, it is not surprising to see tight agreement in beam calibration with cylindrical chambers at 6 MV (0.6% spread). At 18 MV the 1.3% spread would become as tight as that for 6 MV if Seuntjens *et al.*[3] measured k_Q for Capintec chambers was used. With TG21 for both photons and electrons, and with TG51 for electrons, the spread in the data is up to 2%. Although TG51 discourages the use of clyindrical chambers for low energy electron beams, we did use them for the 6 MeV beam. The average value of the beam output determined by the cylindrical chambers is 0.4% less than the average output determined for plane-parallel chambers calibrated by "calib in e$^-$ beam." This is a small deviation but is consistent with the anticipated systematic error introduced by the thimble dimensions and the sharpness of the electron depth-dose peak.

Now the discussion switches to PP chambers, where the issue is complicated by the two techniques of chamber calibration. For chambers calibrated using technique (i), "^{60}Co calib," the 2%–2.5% spread among electron results for PP chambers is marginally larger than those for cylindrical results using both TG51 and TG21. Our data shows a consistent disagreement between PP and cylindrical results. PP chambers determine 1.5%–2% higher output than cylindrical

chambers for electrons, and 2% lower output for photons with either protocol. Technique (ii) "calib in e^- beam," by definition, normalizes the PP results to cylindrical results at the high energy used for the cross comparison. The question then remains twofold as the beam energy changes; how well the agreement among the PP chambers continues, and how well the agreement with the cylindrical chamber continues. Our results at 6 MeV are very positive in both regards. The spread in PP results is small (0.3%) and the outliers are only ~0.5% different. The 0.4% agreement with cylindrical chambers is already discussed above. We do need to remember that the small spread among PP chambers (Figs. 6 and 7) is deceptive. The displayed PP results are based on cross comparison with only one cylindrical chamber. As the PP chambers could have been compared with any other of the cylindrical chambers, the spread of the cylindrical chambers must be added to the apparent spread of the PP results. The worst agreement between PP and cylindrical chambers seen in this work is with TG21 for photons when the plane-parallel chambers are calibrated with technique (ii), "calib in e- beam."

Our results therefore, indicate strong support for the TG51 recommendations that PP chambers not be used for photon beams and that calibration technique (ii) is preferred over technique (i). The ADCL calibration of a PP chamber may continue to prove useful as a redundant check and to satisfy regulatory requirements.

ACKNOWLEDGMENTS

The authors acknowledge the contribution of Peter Balter who developed the software to capture data simultaneously for up to 5 chambers; without which our job would have been even more tedious; and to David W.O. Rogers (formerly at NRC of Canada) for thoughtful consultation on many issues. The authors also acknowledge Leon Eglezopolous of Scanditronics (Wellhofer), Leroy Humphries of CNMC Corporation, Steven Kirsner of MDACC Bellaire Radiation Oncology, and Stephen Szeglin of PTW New York for lending us various ion chambers in this study. The authors also wish to acknowledge the assistance of Elizabeth Siller for processing this paper to make it presentable.

[1]P. R. Almond, P. J. Biggs, B. M. Coursey, W. F. Hanson, M. S. Huq, R. Nath, and D. W. O. Rogers, "AAPM's TG-51 Protocol for clinical reference dosimetry of high-energy photon and electron beams," Med. Phys. **26**, 1847–1870 (1999).

[2]AAPM TG-21, "A protocol for the determination of absorbed dose from high-energy photon and electron beams," Med. Phys. **10**, 741–771 (1983).

[3]J. P. Seuntjens, C. K. Ross, K. R. Shortt, and D. W. O. Rogers, "Absorbed dose beam quality conversion factors for cylindrical chambers in high energy photon beams," Med. Phys. **27**, 2763–2779 (2000).

[4]P. R. Almond, F. H. Attix, L. J. Humphries, H. Kubo, R. Nath, S. Goetsch, and D. W. O. Rogers, "The calibration and use of plane-parallel ionization chambers for dosimetry of electron beams: An extension of the 1983 AAPM protocol report of AAPM Radiation Therapy Committee Task Group No. 39," Med. Phys. **21**, 1251–1260 (1994).

[5]R. C. Tailor and W. F. Hanson, "Calculated absorbed dose ratios, TG51/TG21, for most widely used cylindrical and parallel-plate chambers over a range of photon and electron energies," Med. Phys. **29**, 1454–1472 (2002).

[6]IAEA, "Absorbed dose determination in photon and electron beams," *An International Code of Practice, Technical Report Series* (IAEA, Vienna, 1987), Vol. 277.

[7]D. W. O. Rogers, "Fundamentals of dosimetry based on absorbed dose standards," *Proceedings of the AAPM 1996 summer school, Teletherapy: present and future*, 1996, pp. 319–356.

[8]D. W. O. Rogers, "Approach to electron beam reference dosimetry," Med. Phys. **25**, 310–320 (1998).

[9]E. Mainegra-Hing, I. Kawrakow, and D. W. O. Rogers, "Calculations for plane parallel ion chambers in cobalt 60 beams using the EGSnrc code," Med. Phys. **30**, 179–189 (2003).

[10]R. Nath and R. J. Schulz, "Calculated response and wall correction factors for ionization chambers exposed to ^{60}Co gamma-rays," Med. Phys. **8**, 85–93 (1981).

[11]R. Gastorf, L. J. Humphries, and M. L. Rozenfeld, "Cylindrical chamber dimensions and other data values," Med. Phys. **13**, 751–754 (1986).